Generalized harmonic spatial coordinates and hyperbolic shift conditions

Miguel Alcubierre,[1] Alejandro Corichi,[1] José A. González,[2] Darío Núñez,[1] Bernd Reimann,[1,3] and Marcelo Salgado[1]

[1]*Instituto de Ciencias Nucleares, Universidad Nacional Autónoma de México, A.P. 70-543, México D.F. 04510, México*

[2]*Theoretical Physics Institute, University of Jena, Max-Wien-Platz 1, 07743, Jena, Germany*

[3]*Max Planck Institut für Gravitationsphysik, Albert Einstein Institut, Am Mühlenberg 1, 14476 Golm, Germany*

(Received 1 July 2005; revised manuscript received 24 October 2005; published 16 December 2005)

We propose a generalization of the condition for harmonic spatial coordinates analogous to the generalization of the harmonic time slices introduced by Bona *et al.*, and closely related to dynamic shift conditions recently proposed by Lindblom and Scheel, and Bona and Palenzuela. These generalized harmonic spatial coordinates imply a condition for the shift vector that has the form of an evolution equation for the shift components. We find that in order to decouple the slicing condition from the evolution equation for the shift it is necessary to use a rescaled shift vector. The initial form of the generalized harmonic shift condition is not spatially covariant, but we propose a simple way to make it fully covariant so that it can be used in coordinate systems other than Cartesian. We also analyze the effect of the shift condition proposed here on the hyperbolicity of the evolution equations of general relativity in $1 + 1$ dimensions and $3 + 1$ spherical symmetry, and study the possible development of blowups. Finally, we perform a series of numerical experiments to illustrate the behavior of this shift condition.

DOI: 10.1103/PhysRevD.72.124018 PACS numbers: 04.25.Dm, 04.20.Ex, 95.30.Sf

I. INTRODUCTION

When one studies the time evolution of the gravitational field in general relativity, a good choice of coordinates (a ''gauge'' choice) can make the difference between finding a well behaved solution for a large portion of the spacetime, or running into a coordinate (or physical) singularity in a finite coordinate time, which would not allow a numerical evolution to continue any further. In the $3 + 1$ formulation, the choice of the time coordinate is related with the lapse function, while the choice of the spatial coordinates is related to the shift vector. Many different ways to choose the lapse and the shift have been proposed and used in numerical simulations in the past (see, for example, the pioneering papers of Smarr and York [1,2]). Some gauge choices involve solving elliptic equations, while others involve solving evolution type equations, which may or may not be hyperbolic in character. Recently, hyperbolic coordinate conditions have become a focus of attention, as they in principle allow one to write the full set of dynamical equations as a well-posed system [3–8], while at the same time being both easier to implement and considerably less computationally expensive than elliptic conditions.

The classic example of hyperbolic coordinate conditions are the so-called harmonic coordinates, which are defined by asking for the wave operator acting on the coordinate functions x^μ to vanish. Harmonic coordinate conditions have the important property of allowing the Einstein field equations to be written as a series of wave equations (with nonlinear source terms) for the metric coefficients $g_{\mu\nu}$. Because of this, these conditions were used to prove the first theorems on the existence of solutions to the Einstein equations [9]. This property of transforming the Einstein equations into wave equations could in principle also be seen as an important advantage in the numerical integration of these equations. Still, with few exceptions (see for example [10–12]), full harmonic coordinates have traditionally not been used in numerical relativity, though harmonic time slices have been advocated and used in some cases [13–16]. The reason for this is twofold: In the first place, harmonic coordinates are rather restrictive, and formulations of the Einstein equations for numerical relativity are usually written in a way that allows the gauge freedom to remain explicit so it can be used to control certain aspects of the evolution (avoid singularities, enforce symmetries, reduce shear, etc.). Also, in the particular case of a harmonic time coordinate, it has been shown that the spacelike foliation avoids focusing singularities only marginally, and is therefore not a good choice in many cases [5,13,17,18]. Of course, it can be argued that any coordinate choice is harmonic if one does not ask for the wave operator acting on the coordinate functions to be zero, but instead to be equal to a known function of spacetime (a ''gauge source function''). This is certainly true, but of little use in real life numerical simulations where there is no way to know *a priori* what is a convenient choice for these gauge source functions (but see [12] for some suggestions that seem to work well in practice).

Nevertheless, the fact that the use of harmonic coordinates allows the field equations to be written in strongly hyperbolic form makes one immediately ask if there might be simple generalizations of the harmonic conditions that will still allow the field equations to be written in strongly hyperbolic form, while at the same time retaining a useful degree of gauge freedom. That this is indeed the case was first shown for the particular case of a harmonic time coordinate by Bona *et al.* in [19], where a strongly hyperbolic reformulation of the Einstein evolution equations was constructed using a generalized harmonic slicing condition

which is usually referred to as the Bona-Masso slicing condition. It includes as particular cases several gauge choices that had been used in numerical simulations from the early 90's with good results, such as, for example, the "1 + log" slicing [20,21]. In fact, the Bona-Masso slicing condition was motivated precisely to include such empirically tested conditions in a strongly hyperbolic formulation of the Einstein equations.

In this paper we want to follow a similar approach and propose a generalization of the harmonic spatial coordinate condition. We will show how this allows us to obtain a hyperbolic shift condition that is very closely related to conditions already proposed in the literature, most notably the shift conditions recently introduced by Lindblom and Scheel [8], and by Bona and Palenzuela [22] (in fact, under some specific circumstances, one finds that the shift condition proposed here becomes a particular case of those of Refs. [8,22]).

This paper is organized as follows. In Sec. II we discuss the standard harmonic coordinates and write them as evolution equations for the lapse and shift. We also introduce a rescaled shift vector that allows one to decouple the lapse and shift equations. Section III generalizes the condition for spatial harmonic coordinates, and Sec. IV discusses the interpretation of this condition in curvilinear coordinate systems. In Sec. V we describe the concept of hyperbolicity and the source criteria for avoiding blowups. Section VI studies the generalized harmonic shift condition in the case of 1 + 1 dimensions, analyzing its hyperbolicity properties, the possible appearance of blowups ("gauge shocks"), and also the behavior of this shift condition in numerical simulations. In Sec. VII we repeat the same type of analysis for spherical symmetry and again present results from numerical simulations. We conclude in Sec. VIII. Finally, the appendix shows a formal derivation of the generalized harmonic lapse and shift conditions.

II. HARMONIC COORDINATES

Let us consider four scalar coordinate functions ϕ^α defined on a given background spacetime. The condition for these coordinates to be harmonic is simply

$$\Box\phi^\alpha := g^{\mu\nu}\nabla_\mu\nabla_\nu\phi^\alpha = 0, \tag{2.1}$$

with $g_{\mu\nu}$ the spacetime metric tensor.

Let us further assume that ϕ^0 is such that its level surfaces are spacelike. In that case, ϕ^0 can be identified with a global time function. If we define the lapse function α as the interval of proper time when going from the hypersurface $\phi^0 = t$ to the hypersurface $\phi^0 = t + dt$ along the normal direction, then it is easy to show that α will be given in terms of ϕ^0 as

$$\alpha = (-\nabla\phi^0 \cdot \nabla\phi^0)^{-1/2}. \tag{2.2}$$

The definition of the shift vector is somewhat more involved. We start by defining three scalar functions β^a such that when we move from a given level surface of ϕ^0 to the next following the normal direction, the change in the spatial coordinate functions ϕ^a is given by

$$\phi^a_{t+dt} = \phi^a_t - \beta^a d\phi^0, \tag{2.3}$$

from which one can easily find

$$\beta^a = -\alpha(\vec{n} \cdot \nabla\phi^a), \tag{2.4}$$

with $\vec{n}$ the unit normal vector to the hypersurface $\phi^0 = t$,

$$\vec{n} = -\alpha\nabla\phi^0, \tag{2.5}$$

and where the minus sign is there to guarantee that $\vec{n}$ is future pointing. Thus defined, the β^a are scalars, but we can use them to define a vector $\vec{\beta}$ by asking for its components in the coordinate system $\{\phi^\alpha\}$ to be given by $(0, \beta^a)$. The vector constructed in this way is clearly orthogonal to $\vec{n}$. In an arbitrary coordinate system $\{x^\mu\}$, the shift components will then be given by

$$\beta^\mu = -\alpha(\vec{n} \cdot \nabla\phi^a)\frac{\partial x^\mu}{\partial\phi^a}. \tag{2.6}$$

Notice that with this definition, the shift vector is proportional to the lapse function, so that a simple rescaling of ϕ^0 changes the shift. This suggests that it is perhaps more natural to define a rescaled shift vector $\vec{\sigma}$ in the following way

$$\sigma^\mu := \frac{\beta^\mu}{\alpha} = -(\vec{n} \cdot \nabla\phi^a)\frac{\partial x^\mu}{\partial\phi^a}. \tag{2.7}$$

We will see below that this rescaled shift vector will be important when expressing the harmonic condition in 3 + 1 language.

The harmonic coordinate conditions can be simplified by expanding them in the coordinate system $\{x^\alpha = \phi^\alpha\}$, in which case they reduce to

$$\Gamma^\alpha := g^{\mu\nu}\Gamma^\alpha_{\mu\nu} = 0, \tag{2.8}$$

where $\Gamma^\alpha_{\mu\nu}$ are the Christoffel symbols associated with the 4-metric $g_{\mu\nu}$. If we now relate the coordinates $\{x^\alpha = \phi^\alpha\}$ to the standard 3 + 1 coordinates, then these four equations can be shown to become (see the appendix)

$$\partial_t\alpha = \beta^a\partial_a\alpha - \alpha^2 K, \tag{2.9}$$

$$\partial_t\beta^i = \beta^a\partial_a\beta^i - \alpha\partial^i\alpha + \alpha^2\,{}^{(3)}\Gamma^i + \frac{\beta^i}{\alpha}(\partial_t\alpha - \beta^a\partial_a\alpha + \alpha^2 K). \tag{2.10}$$

Here K is the trace of the extrinsic curvature, and ${}^{(3)}\Gamma^i$ is defined in terms of the three-dimensional Christoffel symbols ${}^{(3)}\Gamma^i_{jk}$, the spatial metric γ_{ij} and its determinant $\gamma := \det\gamma_{ij}$ by ${}^{(3)}\Gamma^i := \gamma^{jk}{}^{(3)}\Gamma^i_{jk} = -\partial_j(\sqrt{\gamma}\gamma^{ij})/\sqrt{\gamma}$. Notice that in Eq. (2.10) we have an explicit dependency on the time derivative of the lapse function. This dependency is

usually not written down, as the whole last term of the second equation vanishes if the first equation is assumed to hold, but we prefer to leave the dependency explicit (see for example [11,23]; incidentally, Eq. (2.10) fixes a sign error in [23], and includes a term missing in [11]).

The fact that the evolution equation for the shift depends on the time derivative of the lapse is inconvenient if one wants to use harmonic spatial coordinates with a different slicing condition, say maximal slicing. It is also an indication that the shift itself might not be the most convenient function to evolve. Remarkably, it turns out that if we rewrite the evolution equation for the shift in terms of the rescaled shift $\sigma^i = \beta^i/\alpha$ introduced above, then the spatial harmonic condition decouples completely from the evolution of the lapse. We find

$$\partial_t \sigma^i = \alpha \sigma^a \partial_a \sigma^i - \partial^i \alpha + \alpha(\sigma^i K + {}^{(3)}\Gamma^i). \tag{2.11}$$

Therefore, if one works with σ^i instead of β^i, one can use harmonic spatial coordinates with an arbitrary slicing condition in a straightforward way.

A final comment about Eqs. (2.9) and (2.10) is in order. Equation (2.9) is clearly a scalar equation as seen in the spatial hypersurfaces. Equation (2.10), on the other hand, is not 3-covariant, i.e. starting from exactly the same 3-geometry but in different coordinates, it will produce a different evolution for the shift vector. This might seem surprising since this equation is just the 3 + 1 version of the condition for spatial harmonic coordinates which is 4-covariant. However, there is no real contradiction, since changing the coordinates on the spatial hypersurfaces means changing the scalar functions ϕ^i themselves, so it should not be surprising that we get a different shift. We will come back to this point in Sec. IV, where we will propose a way to make the shift evolution equation fully 3-covariant.

III. GENERALIZED HARMONIC COORDINATES

In [19], Bona *et al.* generalize the harmonic slicing condition (2.9) in the following way

$$\partial_t \alpha - \beta^a \partial_a \alpha = -\alpha^2 f(\alpha) K, \tag{3.1}$$

with $f(\alpha)$ a positive but otherwise arbitrary function of the lapse. This slicing condition was originally motivated by the Bona-Masso hyperbolic reformulation of the Einstein equations [14,15,18,19,24], but it can in fact be used with any form of the 3+1 evolution equations. As discussed in [5], the Bona-Masso slicing condition above can be shown to avoid both focusing singularities [18] and gauge shocks [25] for particular choices of f. Reference [5] also shows that condition (3.1) can be written in 4-covariant form in terms of a global time function ϕ^0 as

$$(g^{\mu\nu} - a_f n^\mu n^\nu)\nabla_\mu \nabla_\nu \phi^0 = 0, \tag{3.2}$$

with $a_f := 1/f(\alpha) - 1$ and n^μ the unit normal vector to the spatial hypersurfaces defined in (2.5). Here we will introduce an analogous generalization of the spatial harmonic coordinates $\{\phi^l\}$. That is, we propose the following spatial gauge condition

$$(g^{\mu\nu} - a_h n^\mu n^\nu)\nabla_\mu \nabla_\nu \phi^l = 0, \tag{3.3}$$

where n^μ is still the unit normal to the spatial hypersurfaces, but now $a_h := 1/h - 1$, with $h(\alpha, \beta^i)$ a scalar function that can in principle depend on both the lapse and shift (we will see below that the shift dependence is in fact not convenient). In the coordinate system $\{x^\mu = \phi^\mu\}$, condition (3.3) becomes

$$(g^{\mu\nu} - a_h n^\mu n^\nu)\Gamma^l_{\mu\nu} = 0. \tag{3.4}$$

Expressing the 4-metric and normal vector in terms of 3+1 variables, the last equation becomes

$$\Gamma^l_{00} - 2\beta^m \Gamma^l_{m0} + \beta^m \beta^n \Gamma^l_{mn} = \alpha^2 h \gamma^{mn} \Gamma^l_{mn}. \tag{3.5}$$

Notice that on the right-hand side of this equation appears the contraction $\gamma^{mn}\Gamma^l_{mn}$ which should not be confused with $\Gamma^l := g^{\mu\nu}\Gamma^l_{\mu\nu}$. Inserting now the expressions for the Γ^l_{mn} in terms of $3 + 1$ quantities we obtain (see also the appendix)

$$\partial_t \beta^l = \beta^m \partial_m \beta^l - \alpha \partial^l \alpha + \frac{\beta^l}{\alpha}(\partial_t \alpha - \beta^m \partial_m \alpha) + \alpha^2 h\left(\frac{\beta^l}{\alpha} K + {}^{(3)}\Gamma^l\right). \tag{3.6}$$

This is to be compared with Eq. (2.10) of the previous section. Notice that again we find that the evolution equation for the shift is coupled to that of the lapse. In the same way as before, we can decouple the shift evolution equation by writing it in terms of the rescaled shift $\sigma^i = \beta^i/\alpha$. We find

$$\partial_t \sigma^l = \alpha \sigma^m \partial_m \sigma^l - \partial^l \alpha + \alpha h(\sigma^l K + {}^{(3)}\Gamma^l), \tag{3.7}$$

which is to be compared with (2.11). This is the final form of the condition for generalized harmonic spatial coordinates, and we will refer to this condition simply as the "generalized harmonic shift" (but see Sec. IV below where the condition is somewhat modified to make it fully 3-covariant).

At this point it is important to discuss the relation that the shift condition (3.6) has with the conditions recently proposed by Lindblom and Scheel [8], and by Bona and Palenzuela [22]. It is not difficult to see that by choosing the free parameters in these references appropriately, one can in fact recover condition (3.6), but only *provided* one also takes the lapse to evolve via the Bona-Masso slicing condition (3.1) and takes $f = h$. If, on the other hand, one uses a different slicing condition (say maximal slicing), or uses the Bona-Masso slicing condition with $f \neq h$, then this is no longer the case and the shift condition proposed here will differ from those of Refs. [8,22]. This is a crucial point, and shows the importance of rescaling the shift in

order to decouple its evolution equation from the time derivative of the lapse.

In the following sections we will study this shift condition. We will first discuss the issue of the interpretation of the generalized harmonic shift condition for curvilinear coordinates in Sec. IV. Later, in Sec. V we will introduce the concept of hyperbolicity, and a criteria for avoiding blowups in the solutions of strongly hyperbolic systems of equations. Finally, in Secs. VI and VII we will consider the special cases of 1+1 dimensional relativity and spherical symmetry. In each case we will analyze the hyperbolicity properties of the full system of equations *including* the generalized harmonic shift condition, study the possible development of blowups, and present a series of numerical examples.

IV. CURVILINEAR VERSUS CARTESIAN COORDINATES

We have already mentioned that the harmonic shift condition (2.11), and its generalization (3.7), are in fact not covariant with respect to changes in the spatial coordinates. That is, starting from exactly the same 3-geometry but with different spatial coordinates we will get a different evolution of the shift vector. In particular, for curvilinear systems of coordinates one could find that even starting from a flat slice of Minkowski spacetime we would still have nontrivial shift evolution driven by the fact that the initial ${}^{(3)}\Gamma^i$ do not vanish (i.e. the spatial curvilinear coordinates are not 3-harmonic). Worse still, in many cases it can happen that the ${}^{(3)}\Gamma^i$ of flat space are not only nonzero but are also singular, as is the case with spherical coordinates for which ${}^{(3)}\Gamma^r$ is of order $1/r$. One may also find that in physical systems that have a specific symmetry the shift evolution will break the symmetry because of the properties of some of the ${}^{(3)}\Gamma^i$. An example of this are again spherical coordinates for which one finds that ${}^{(3)}\Gamma^\theta \neq 0$, so σ^θ will evolve away from zero even for a spherically symmetric system.

The question then arises how to interpret the harmonic shift condition in a general coordinate system, and, in particular, how to make sure that we do not run into pathological situations like those described above. Our proposal for resolving this issue is to always apply the generalized harmonic shift condition in a coordinate system that is topologically Cartesian. Of course, if one has a situation that has a specific symmetry, one would like to work with a coordinate system that is adapted to that symmetry. We therefore need to transform condition (3.7) from Cartesian coordinates to our curvilinear coordinates, but taking into account the fact that the condition is not covariant.

Let us denote by $\{x^{\bar{a}}\}$ our reference topologically Cartesian coordinates, and by $\{x^i\}$ the general curvilinear coordinates. If we assume that condition (3.7) is satisfied for the original coordinates $\{x^{\bar{a}}\}$ we will have

$$\partial_t \sigma^{\bar{a}} = \alpha \sigma^{\bar{b}} \partial_{\bar{b}} \sigma^{\bar{a}} - \partial^{\bar{a}} \alpha + \alpha h(\sigma^{\bar{a}} K + {}^{(3)}\Gamma^{\bar{a}}). \quad (4.1)$$

In order to transform this expression we will use the fact that with respect to the 3-geometry σ^i behaves like a vector, while α and K behave as scalars. Remembering now that the Christoffel symbols transform as

$${}^{(3)}\Gamma^i_{jk} = (\partial_{\bar{a}} x^i \partial_j x^{\bar{b}} \partial_k x^{\bar{c}}) {}^{(3)}\Gamma^{\bar{a}}_{\bar{b}\,\bar{c}} + F^i_{jk}, \quad (4.2)$$

with $F^i_{jk} := \partial_{\bar{a}} x^i \partial_j \partial_k x^{\bar{a}}$, we find that in the curvilinear coordinate system Eq. (4.1) becomes

$$\partial_t \sigma^l = \alpha \sigma^m \partial_m \sigma^l + \alpha \sigma^m \sigma^n F^l_{mn} - \partial^l \alpha + \alpha h(\sigma^l K + {}^{(3)}\Gamma^l - \gamma^{mn} F^l_{mn}). \quad (4.3)$$

By rearranging some terms, the shift condition can finally be written in the more convenient form

$$\partial_t \sigma^l = \alpha \sigma^m \nabla_m \sigma^l - \nabla^l \alpha + \alpha h \sigma^l K + \alpha(h\gamma^{mn} - \sigma^m \sigma^n)\Delta^l_{mn}, \quad (4.4)$$

with $\Delta^l_{mn} := {}^{(3)}\Gamma^l_{mn} - F^l_{mn}$. The last expression is in fact 3-covariant, as one can readily verify that the Δ^l_{mn} transform as the components of a 3-tensor. But the price we have paid is that we have chosen a privileged coordinate system to be used as a reference in order to define F^l_{mn}. It is clear that for the original coordinates $\{x^{\bar{a}}\}$ the condition above reduces to what we had before since F^l_{mn} vanishes. We will consider the case of spherical coordinates in Sec. VII below.

In practice, one can use the fact that for flat space in Cartesian coordinates the Christoffel symbols vanish, which implies

$$F^l_{mn} = {}^{(3)}\Gamma^l_{mn}|_{\text{flat}}, \quad (4.5)$$

so that

$$\Delta^l_{mn} = {}^{(3)}\Gamma^l_{mn} - {}^{(3)}\Gamma^l_{mn}|_{\text{flat}}. \quad (4.6)$$

V. HYPERBOLICITY AND SHOCKS

A. Hyperbolic systems

The concept of hyperbolicity is of fundamental importance in the study of the evolution equations associated with a Cauchy problem as the initial value problem for strongly or symmetric hyperbolic systems can be shown to be well-posed (though the well-posedness of strongly hyperbolic systems requires that some additional smoothness conditions are verified). In the following we will concentrate on one-dimensional systems, for which the distinction between strongly and symmetric hyperbolic systems does not arise.

Following [26], we will consider quasilinear systems of evolution equations that can be split into two subsystems of the form

$$\partial_t u = \mathbf{M}(u) v, \quad (5.1)$$

$$\partial_t \boldsymbol{v} + \mathbf{A}(u)\partial_x \boldsymbol{v} = q_v(u, \boldsymbol{v}). \tag{5.2}$$

Here u and $\boldsymbol{v}$ are n and m dimensional vector-valued functions, and $\mathbf{M}$ and $\mathbf{A}$ are $n \times n$ and $m \times m$ matrices, respectively. In addition we demand that the $\boldsymbol{v}$'s are related to either time or space derivatives of the u's. This implies that derivatives of the u's can always be substituted for $\boldsymbol{v}$'s and hence treated as source terms.

The system of equations above will be hyperbolic if the matrix $\mathbf{A}$ has m real eigenvalues λ_i. Furthermore, it will be strongly hyperbolic if it has a complete set of eigenvectors $\vec{\xi}_i$. If we denote the matrix of column eigenvectors by $\mathbf{R} = (\vec{\xi}_1 \cdots \vec{\xi}_m)$, then the matrix $\mathbf{A}$ can be diagonalized as

$$\mathbf{R}^{-1}\mathbf{A}\mathbf{R} = \mathbf{diag}[\lambda_1, \cdots, \lambda_m] = \Lambda. \tag{5.3}$$

For a strongly hyperbolic system we then define the eigenfields as

$$w = \mathbf{R}^{-1}\boldsymbol{v}. \tag{5.4}$$

By analyzing the time evolution of the eigenfields, one can identify mechanisms that lead to blowups in the solution, which in [27] have been referred to as ''geometric blowup'' (leading to ''gradient catastrophes'' [28]) and the ''ODE-mechanism'' (causing ''blowups within finite time''). In [26] some of us presented blowup avoiding conditions for both these mechanisms, which we called ''indirect linear degeneracy'' [25] and the ''source criteria.'' In that reference it was also shown, using numerical examples, that the source criteria for avoiding blowups is generally the more important of the two conditions. Because of this, and also because of the fact that the true relevance of indirect linear degeneracy is not as yet completely clear, in this paper we will concentrate only on the source criteria.

B. Source criteria for avoiding blowups

An evolution variable can become infinite at a given point by a process of ''self-increase'' in the causal past of this point. A criteria to avoid such blowups for systems of partial differential equations of the form (5.1) and (5.2) was proposed by some of us in [26]: When diagonalizing the evolution system for the $\boldsymbol{v}$'s, making use of (5.3) and (5.4), one finds

$$\partial_t w + \Lambda\partial_x w = q_w, \tag{5.5}$$

where

$$q_w := \mathbf{R}^{-1}q_v + [\partial_t\mathbf{R}^{-1} + \Lambda\partial_x\mathbf{R}^{-1}]\boldsymbol{v}. \tag{5.6}$$

This yields an evolution system where on the left-hand side of (5.5) the different eigenfields w_i are decoupled. However, in general the equations are still coupled through the source terms q_{w_i}. In particular, if the original sources were quadratic in the $\boldsymbol{v}$'s, one obtains

$$\frac{dw_i}{dt} = \partial_t w_i + \lambda_i\partial_x w_i = \sum_{j,k=1}^{m} c_{ijk}w_j w_k + \mathcal{O}(w), \tag{5.7}$$

where $d/dt := \partial_t + \lambda_i\partial_x$ denotes the derivative along the corresponding characteristic. As pointed out in [26], the $c_{iii}w_i^2$ component of the source term can be expected to dominate and to cause blowups in the solution within a finite time. In order to avoid these blowups we therefore demand that the coefficients c_{iii} should vanish, and we refer to this condition as the ''source criteria.''

It is not difficult to convince oneself that the source criteria is in fact not a sufficient condition for avoiding blowups, as already discussed in [26]. However, one can still expect the source criteria to be a necessary condition for avoiding blowups at least for small perturbations propagating with different eigenspeeds, as mixed terms will be suppressed when pulses moving at different speeds separate from each other, while the effect of the term w_i^2 will remain as each pulse moves. If, however, some eigenfields w_i and w_j travel with identical or similar eigenspeeds, then one should also expect important contributions coming from the mixed terms $w_i w_j$. We will show an example later on where eliminating such mixed terms (in addition to the quadratic terms) indeed leads to further improvements.

VI. EINSTEIN EQUATIONS IN 1 + 1 DIMENSIONS

We first consider standard general relativity in one spatial dimension (and in vacuum). Since in this paper we are interested precisely in studying a new shift condition, 1 + 1 dimensional relativity is an ideal testing ground for the ''gauge dynamics'' which one can expect in the higher dimensional case.

In the following sections we will introduce the evolution equations and gauge conditions, and consider the possible formation of blowups associated with our gauge conditions. We will also present numerical simulations that show how the generalized harmonic shift condition behaves in practice.

A. Evolution equations

We will start from the ''standard'' Arnowitt-Deser-Misner (ADM) equations for one spatial dimension [29] as formulated in [23]. In this case the u quantities consist of the lapse function α, the rescaled shift $\sigma := \sigma^x$, and the spatial metric function $g := g_{xx}$. The $\boldsymbol{v}$ quantities, on the other hand, are given by the spatial derivatives of the u's and, in addition, the unique component of the extrinsic curvature. That is,

$$u = (\alpha, \sigma, g), \qquad \boldsymbol{v} = (D_\alpha, d_\sigma, D_g, \tilde{K}), \tag{6.1}$$

with $\tilde{K} := \sqrt{g}\,\mathrm{tr}K = \sqrt{g}K^x_x$, and where we have defined

$$D_\alpha := \partial_x \ln\alpha, \qquad D_g := \partial_x \ln g, \qquad d_\sigma := \partial_x\sigma. \tag{6.2}$$

Notice first that we use a rescaled extrinsic curvature, as

this makes the evolution equations considerably simpler. Also, we use logarithmic spatial derivatives of α and g, but only the ordinary spatial derivative of the rescaled shift σ, as the shift is allowed to change sign.

For the evolution of the gauge variables we will use the Bona-Masso slicing condition (3.1) and the generalized harmonic shift condition (3.7). The equations for the u's are then

$$\partial_t \alpha = \alpha^2 \Big[\sigma D_\alpha - \frac{f\tilde{K}}{\sqrt{g}} \Big], \tag{6.3}$$

$$\partial_t \sigma = \alpha \Big[\sigma d_\sigma - \frac{D_\alpha}{g} + h\Big(\frac{D_g}{2g} + \frac{\sigma\tilde{K}}{\sqrt{g}} \Big) \Big], \tag{6.4}$$

$$\partial_t g = \alpha g \Big[\sigma D_g + 2\Big(d_\sigma + \sigma D_\alpha - \frac{\tilde{K}}{\sqrt{g}} \Big) \Big], \tag{6.5}$$

where $f = f(\alpha)$ and $h = h(\alpha, \sigma)$. The evolution equations for $\{D_\alpha, d_\sigma, D_g\}$ can be obtained directly from the above equations, while the evolution equation for $\tilde{K}$ comes from the ADM equations and takes the following simple form

$$\partial_t \tilde{K} = \partial_x [\alpha(\sigma\tilde{K} - D_\alpha/\sqrt{g})]. \tag{6.6}$$

The evolution equations for the υ's can then be written in full conservative form $\partial_t \upsilon + \partial_x(\mathbf{A}\upsilon) = 0$, with the characteristic matrix $\mathbf{A}$ given by

$$\mathbf{A} = \begin{pmatrix} -\alpha\sigma & 0 & 0 & \alpha f/\sqrt{g} \\ \alpha/g & -\alpha\sigma & -\alpha h/2g & -\alpha h\sigma/\sqrt{g} \\ -2\alpha\sigma & -2\alpha & -\alpha\sigma & 2\alpha/\sqrt{g} \\ \alpha/\sqrt{g} & 0 & 0 & -\alpha\sigma \end{pmatrix}. \tag{6.7}$$

This matrix has the following eigenvalues

$$\lambda^f_\pm = \alpha(\pm\sqrt{f/g} - \sigma), \tag{6.8}$$

$$\lambda^h_\pm = \alpha(\pm\sqrt{h/g} - \sigma), \tag{6.9}$$

with corresponding eigenfunctions (the normalization is chosen for convenience)

$$w^f_\pm = \tilde{K} \pm D_\alpha/\sqrt{f}, \tag{6.10}$$

$$w^h_\pm = -(1 \pm \sigma\sqrt{gh})\tilde{K} + \sqrt{g} d_\sigma \mp \sqrt{h} D_g/2, \tag{6.11}$$

which can be easily inverted to find

$$D_\alpha = \frac{\sqrt{f}}{2}(w^f_+ - w^f_-), \tag{6.12}$$

$$d_\sigma = \frac{1}{2\sqrt{g}}(w^f_+ + w^f_- + w^h_+ + w^h_-), \tag{6.13}$$

$$D_g = \frac{1}{\sqrt{h}}(w^h_- - w^h_+) - \sigma\sqrt{g}(w^f_+ + w^f_-), \tag{6.14}$$

$$\tilde{K} = \frac{1}{2}(w^f_+ + w^f_-). \tag{6.15}$$

The system is therefore strongly hyperbolic as long as $f > 0$ and $h > 0$, with the lapse and shift eigenfields $w^f_\pm$ and $w^h_\pm$ propagating with the corresponding gauge speeds $\lambda^f_\pm$ and $\lambda^h_\pm$.

B. Gauge shock analysis

By analyzing quadratic source terms in the evolution equations of the eigenfields, we now want to study the possible formation of blowups for the system of evolution equations of the previous section. For the lapse and shift eigenfields we find

$$\frac{dw^f_\pm}{dt} = c^{fff}_{\pm\pm\pm} w^{f2}_\pm + c^{ffh}_{\pm\pm\pm} w^f_\pm w^h_\pm + \mathcal{O}(w^f_\pm w^f_\mp, w^f_\pm w^h_\mp), \tag{6.16}$$

$$\frac{dw^h_\pm}{dt} = c^{hhh}_{\pm\pm\pm} w^{h2}_\pm + c^{hhf}_{\pm\pm\pm} w^h_\pm w^f_\pm + \mathcal{O}(w^h_\pm w^h_\mp, w^h_\pm w^f_\mp). \tag{6.17}$$

In particular, we observe that in (6.16) no term proportional to $w^{h2}_\pm$ is present, and in the same way in (6.17) there is no term proportional to $w^{f2}_\pm$. In order to apply the source criteria we need to calculate those terms quadratic in w_i appearing in the sources of the evolution equation for w_i itself. It turns out that the c_{iii} coefficients have the form

$$c^{fff}_{\pm\pm\pm} \propto (1 - f - \alpha f'/2), \tag{6.18}$$

$$c^{hhh}_{\pm\pm\pm} \propto \partial h/\partial\sigma. \tag{6.19}$$

According to the source criteria these coefficients have to vanish in order to avoid blowups. The conditions on the gauge functions $f(\alpha)$ and $h(\alpha, \sigma)$ are then

$$1 - f - \alpha f'/2 = 0, \tag{6.20}$$

$$\partial h/\partial\sigma = 0. \tag{6.21}$$

The condition (6.20) for $f(\alpha)$ has been studied many times before [5,25,26,30], and its general solution is

$$f(\alpha) = 1 + \text{const.}/\alpha^2. \tag{6.22}$$

For $h(\alpha, \sigma)$, on the other hand, we obtain the condition that h can be an arbitrary function of α, but may not depend on σ, that is, $h = h(\alpha)$.

One now might wonder about the case where h is equal (or very close to) the function f. In that case the eigenfields $w^f_\pm$ and $w^h_\pm$ travel with the same (or similar) eigenspeeds, so mixed terms of the type $w^f_\pm w^h_\pm$ in the sources can be expected to contribute to a blowup. For this reason we have

also calculated the c_{iij} coefficients associated to these terms. Notice, however, that in general the coefficients of such mixed terms are not invariant under rescalings of the eigenfields of the form $\tilde{w}_i = \Omega_i(\alpha, \sigma, g)w_i$, so we have in fact done the calculation assuming an arbitrary rescaling. We find

$$c^{ffh}_{\pm\pm\pm} \propto \left(1 - \sqrt{\frac{h}{f}}\right), \tag{6.23}$$

$$\begin{aligned} c^{hhf}_{\pm\pm\pm} \propto \Bigg\{\Bigg[& 2\alpha\sqrt{f}\frac{\partial\Omega^h_\pm}{\partial\alpha} \pm \frac{2}{\sqrt{g}}\frac{\partial\Omega^h_\pm}{\partial\sigma} \\ & \mp 4\sigma\sqrt{g}\left(\Omega^h_\pm + g\frac{\partial\Omega^h_\pm}{\partial g}\right)\Bigg]\left(1 - \sqrt{\frac{h}{f}}\right) \\ & + \left[\frac{\sqrt{f}}{2h}\left(1 + \sqrt{\frac{h}{f}}\right)\left(\alpha\frac{\partial h}{\partial\alpha} \pm \frac{1}{\sqrt{gf}}\frac{\partial h}{\partial\sigma}\right)\right. \\ & \left. + \frac{1+3h}{\sqrt{h}} - \frac{3+h}{\sqrt{f}}\right]\Omega^h_\pm\Bigg\}. \end{aligned} \tag{6.24}$$

One can readily verify that these coefficients vanish for $f = h = 1 + \text{const.}/\alpha^2$, independently of the rescaling of the eigenfields. This setting of f and h hence seems to be an optimal choice for avoiding blowups.

C. Numerical examples

In order to test the generalized harmonic shift condition we have performed a series of numerical experiments. We evolve Minkowski initial data, but with a nontrivial initial slice given in Minkowski coordinates (t_M, x_M) as $t_M = p(x_M)$, with p a profile function that decays rapidly. If we use $x = x_M$ as our spatial coordinate, the spatial metric and extrinsic curvature turn out to be

$$g(t=0) = 1 - p'^2, \qquad \tilde{K}(t=0) = -p''/g. \tag{6.25}$$

In all the simulations shown below we have taken for the function $p(x)$ a Gaussian centered at the origin

$$p(x) = \kappa \exp\left[-\left(\frac{x}{s}\right)^2\right]. \tag{6.26}$$

For our simulations we have chosen for κ and s the same values used in [25], namely $\kappa = 5$ and $s = 10$. Furthermore, we start with unit lapse and vanishing shift.

All runs have been performed using a method of lines with fourth order Runge-Kutta integration in time, and standard second order centered differences in space. Furthermore, we have used 64 000 grid points and a grid spacing of $\Delta x = 0.0125$ (which places the boundaries at ± 400), together with a time step of $\Delta t = \Delta x/4$. In the simulations shown below, we will concentrate on two different aspects: First, we want to know how the generalized harmonic shift condition works in practice, and what are its effects on the evolution. Also, we want to see if gauge shocks do form when they are expected.

Furthermore, to study the overall growth in the evolution variables, we introduce the quantity δ defined through

$$\delta^2 := (\alpha - 1)^2 + \sigma^2 + (g - 1)^2 + \sum_{i=1}^{4} v_i^2, \tag{6.27}$$

as a measure of how nontrivial the data is. For δ we then also calculate the convergence factor η which, using three runs with high (δ^h), medium (δ^m) and low (δ^l) resolutions differing in each case by a factor of 2, can be calculated by

$$\eta = \frac{\frac{1}{N_i}\sum_{i=1}^{N_i}|\delta^m_i - \delta^l_i|}{\frac{1}{N_j}\sum_{j=1}^{N_j}|\delta^h_j - \delta^m_j|}. \tag{6.28}$$

In the plots we show three different convergence factors. In particular, we denote with a triangle the convergence factor obtained when comparing runs with 64 000, 32 000, and 16 000 grid points and a spatial resolution of 0.0125, 0.25, and 0.5. We then use boxes and diamonds when gradually lowering all three resolutions by a factor of 2. For second order convergence we expect $\eta \simeq 4$.

As a reference of what happens for the case of zero shift, in Fig. 1 we show a run that corresponds to harmonic slicing and vanishing shift (these plots should be compared with Fig. 2 of [25]). In the figures, the initial data is shown as a dashed line, and the final values at $t = 200$ as a solid line (remember that the initial metric is nontrivial).

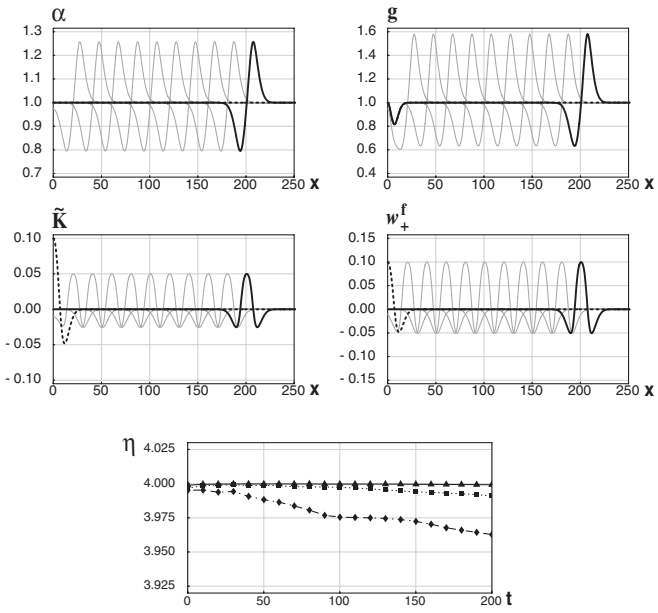

FIG. 1. For a simulation with harmonic slicing ($f = 1$) and vanishing shift, we show the evolution in time of the variables α, g and $\tilde{K}$, together with that of the eigenfield w^f_+. The values of the different quantities are shown every $\Delta t = 20$. In the plot on the bottom we show three convergence factors when increasing the resolution in the order "diamond, box and triangle." In all three cases the convergence factor is close to the expected value of 4.

Intermediate values at intervals of $\Delta t = 20$ are shown in light gray. As can be seen from the plots, all variables behave in a wavelike fashion and the convergence plot indicates that we have close to second order convergence during the whole run for all resolutions considered. Here the pulses are moving out symmetrically in both directions away from the origin (we only show the $x > 0$ side). One can see that the initial nontrivial distortion in g for small x remains (so the dashed and solid lines lie on top of each other there), indicating that even though in the end we return to trivial Minkowski slices, we are left with nontrivial spatial coordinates.

Our second example is shown in Fig. 2 and corresponds to $f = h = 1$, that is, pure harmonic coordinates in both space and time. The simulation is very similar to the previous one and convergences again to second order. The nontrivial shift, however, behaves in such a way that at the end of the run no distortion remains in the metric component g at the origin. One should also note that for $f = h = 1$ both eigenfields propagate with the same speed. However, since quadratic and mixed source terms in the evolution equations of both $w^f_\pm$ and $w^h_\pm$ are not present, simple wavelike behavior for all variables is again observed.

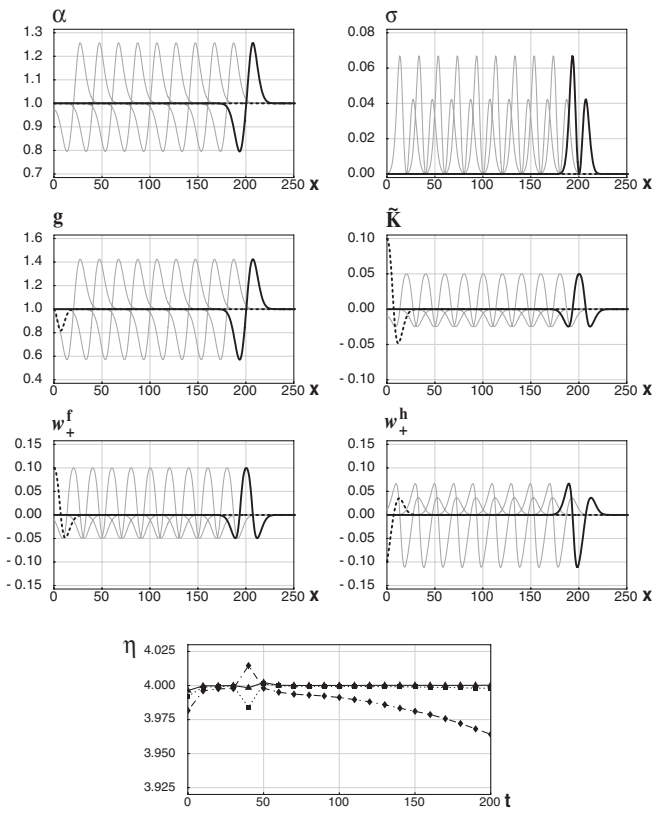

FIG. 2. For a simulation with harmonic slicing and harmonic shift ($f = h = 1$), we show the evolution in time of α, σ, g, and $\tilde{K}$, together with that of w^f_+ and w^h_+. As in the previous figure, the bottom plot shows the convergence factors for different resolutions.

This example allows us to understand the main effect that the introduction of the generalized harmonic shift condition has on the evolution: It drives the spatial coordinates to a situation where no final distortion in the metric is present. In fact, it is not difficult to understand why this is so. From Eq. (4.4) we can see that the sources for the evolution of the rescaled shift are the derivatives of the lapse, the trace of the extrinsic curvature and the Δ^l_{mn}. As the shift condition does not feed back into the slicing condition (apart from a trivial shifting of the time lines), the lapse and the trace of the extrinsic curvature behave just as before, with pulses that propagate away. However, the Δ^l_{mn} will continue to drive the evolution of the shift unless they become zero. The behavior of the shift condition is then to drive the system to a situation where the Δ^l_{mn} vanish. In the simple $1 + 1$ case this is equivalent to reaching a state where the spatial metric itself becomes trivial.

A third example is presented in Fig. 3, which uses again $f = 1$, but now we take $h = 1 + 3\sigma^2$. Initially, the evolution behaves in a very similar way to the previous case. At later times, however, we observe that a sharp gradient

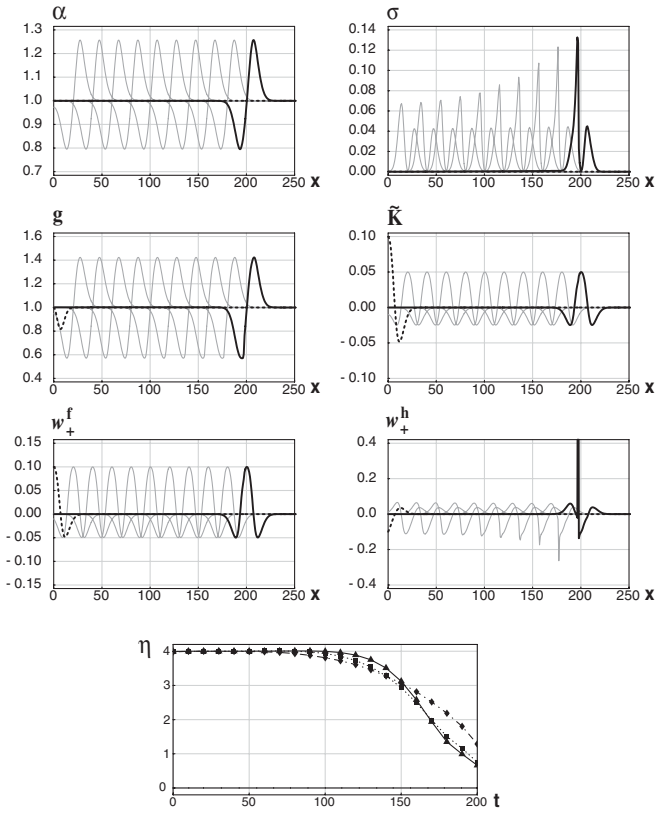

FIG. 3. For $f = 1$ and $h = 1 + 3\sigma^2$, the simulation fails shortly before the time $t = 200$ due to a sharp gradient developing in the rescaled shift σ, and a corresponding large spike appearing in the eigenfield $w^h_\pm$. The bottom plot shows that convergence starts to be lost at $t \simeq 150$ (notice the change of scale as compared to previous plots), indicating that a blowup has happened at around this time. This type of behavior is expected in this case since the source criteria is not satisfied.

develops in the rescaled shift σ, with a corresponding large spike in the shift eigenfield $w^h_\pm$. Moreover, from the convergence plot we see that there is a clear loss of convergence, and as the resolution is increased, this loss of convergence becomes more sharply centered around a specific time $t \simeq 150$, indicating that a blowup happens at this time. Since in this case h is a function of σ, the source criteria is clearly not satisfied. The fact that a large spike has developed in $w^h_\pm$ therefore strengthens the case for the source criteria being a good indicator of when blowups can be expected.

Our final example uses $f = 1$ and $h = 2$, and is shown in Fig. 4. This example is interesting as the speeds for the lapse and shift eigenfields are different. Concentrate first on the evolution of the lapse, the extrinsic curvature and w^f_+. Here the evolution is essentially identical to that of the previous examples, converging again to second order: a pulse travels with roughly unit speed and behind it everything rapidly relaxes back to trivial values. The eigenfield w^h_+, on the other hand, shows a pulse traveling faster, with a speed $\sim\sqrt{2}$. It also takes considerably longer for the region behind this pulse to relax to trivial values. Finally, the metric g and rescaled shift σ separate into two pulses traveling at the two different eigenspeeds. This is to be expected, as from (6.13) and (6.14) we see that metric and shift have contributions from both types of eigenfields.

For the different runs we have also studied the behavior of the logarithm of the root mean square (rms) of δ over time. Since the behavior of the evolution turns out to depend to some extent on the initial data, and, in particular, on the sign of the Gaussian in (6.26), we perform runs for both $\kappa = 5$ and $\kappa = -5$, and then take the average of both runs when calculating δ. For the initial data we are using, at time $t = 0$ this yields a value $\log(\delta) \approx -1.583$ for both signs of κ. In Fig. 5 we plot the rms of the quantity δ for the times $t = \{20, 40, 60, 80, 100\}$, when using either $h = 1$ and varying the (constant) value of f (top panel), or using $f = 1$ together with different (again constant) values of h (bottom panel). From the top panel we see that $f = 1$ is clearly preferred. In addition we want to point out that runs with $f < 0.79$ and $f > 1.25$ crashed before reaching the time $t = 100$. This behavior is expected as we know that constant values of f different from one produce blowups. In the lower panel we observe that for $f = 1$ corresponding to harmonic slicing, $h = 1$ performs best. In addition,

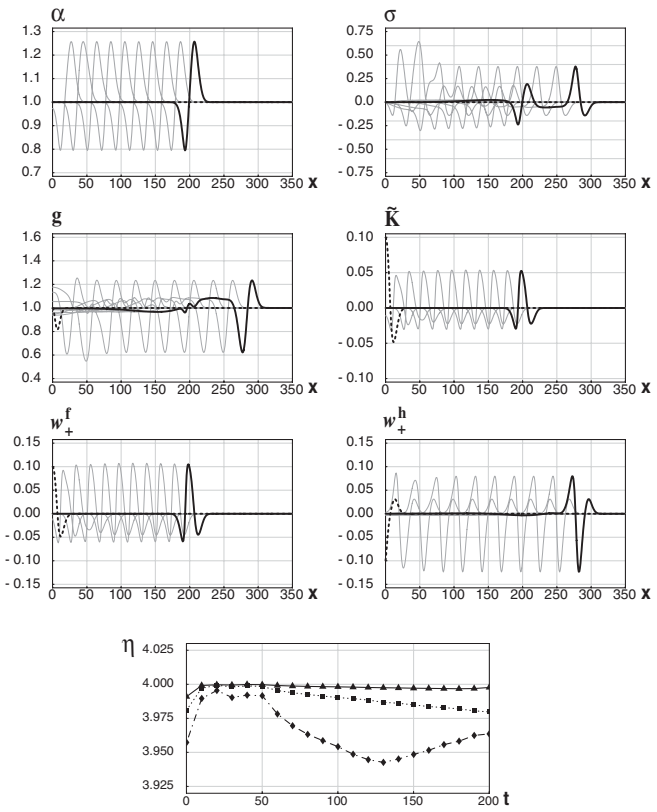

FIG. 4. For $f = 1$ and $h = 2$, the lapse and shift eigenfields travel at different speeds. The lapse, extrinsic curvature and eigenfield w^f_+ show a pulse traveling with roughly unit speed, while the eigenfield w^h_+ shows a pulse moving with speed $\sim\sqrt{2}$. The metric g and rescaled shift σ, on the other hand, separate into two pulses traveling at the two different eigenspeeds.

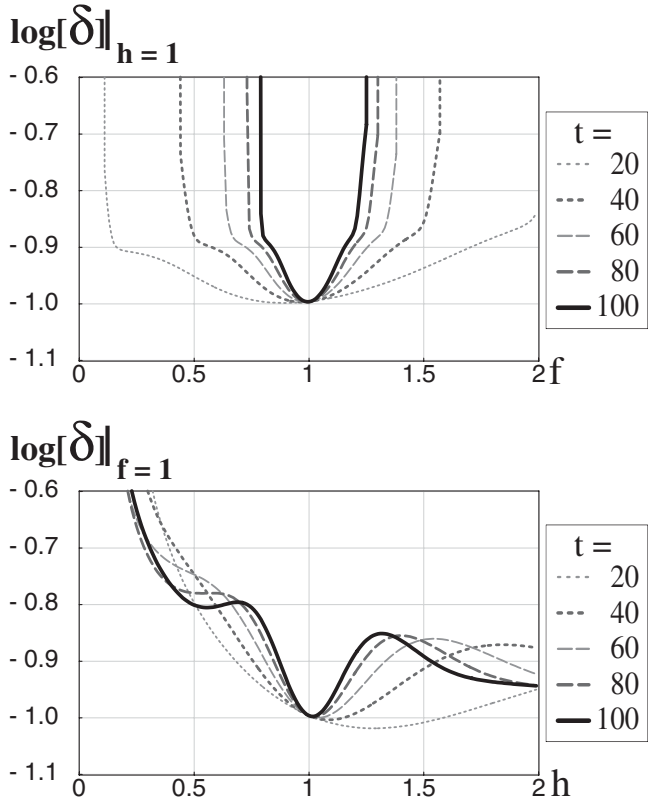

FIG. 5. Top: For evolutions with $h = 1$, the rms of δ is shown on a logarithmic scale as a function of f every $\Delta t = 20$. The value $f = 1$ is obviously preferred. Bottom: For runs with harmonic slicing ($f = 1$), the same quantity is plotted as a function of h. Here $h = 1$ is the optimal choice, but $h \sim 0.5$ or $h \gg 1$ is also preferred.

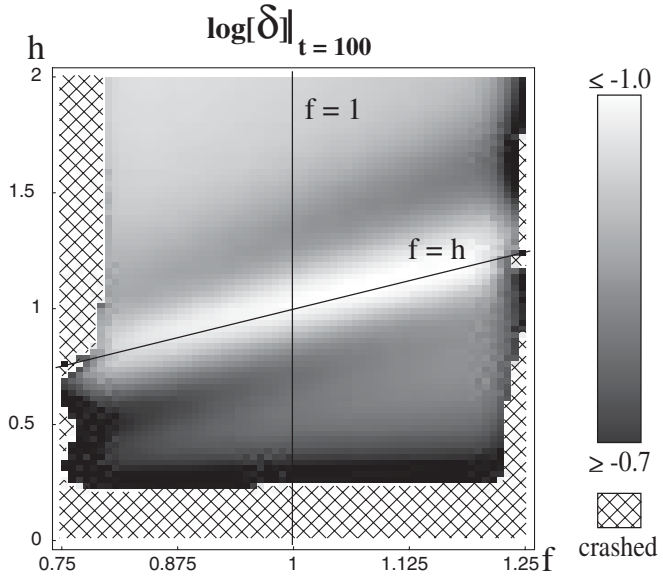

FIG. 6. Contour plot of the rms of δ at time $t = 100$. Small values for this quantity are found for $f = 1$, when $h = 1$ or $h \gg 1$, and also for $f = h$.

values $h \sim 0.5$ and $h \gg 1$ also seem to be preferred. One should note that mixed terms $w^f_\pm w^h_\pm$ in the evolution equations of both $w^f_\pm$ and $w^h_\pm$ for these choices of h play a minor role since localized perturbations in these eigenfields separate quickly when traveling with different speeds. We also want to mention that for $h < 0.19$ the simulations again crashed before reaching the time $t = 100$. The observation that δ grows rapidly and runs crash early if f and/or h are very close to zero can be understood by the fact that the system is not strongly hyperbolic if $f = 0$ and/or $h = 0$.

In the contour plot of Fig. 6 we show the rms of δ at time $t = 100$ as a function of the gauge parameters f and h, using 64×80 equidistant parameter choices. Cases that have already crashed by that time correspond to the hashed regions. Note that the darker regions in this plot denote parameter choices where a significant growth in the evolution variables is present, while brighter regions correspond to runs with very little growth. We find small values for the rms of δ for f being close to its shock avoiding value $f = 1$, and either $h = 1$ or $h \gg 1$. In addition, we can also observe that $f = h$ corresponds to a preferred choice. This can be explained by the fact that for this gauge choice the mixed terms $w^f_\pm w^h_\pm$ are missing in the evolution equations of both $w^f_\pm$ and $w^h_\pm$.

VII. EINSTEIN EQUATIONS IN SPHERICAL SYMMETRY

As a second application of the generalized harmonic shift condition we will consider vacuum general relativity in spherical symmetry. This situation is considerably richer than the $1 + 1$ dimensional case, but it also presents some special problems because of the singular nature of spherical coordinates at the origin.

A. ADM evolution equations

We will consider the spherically symmetric line element written in the form

$$ds^2 = -\alpha^2(1 - A\sigma^2)dt^2 + 2\alpha A\sigma dr dt + A dr^2 + B r^2 d\Omega^2, \tag{7.1}$$

where all the metric coefficients are functions of both t and r. We now introduce the following auxiliary variables

$$D_\alpha := \partial_r \ln\alpha, \qquad d_\sigma := \partial_r \sigma, \tag{7.2}$$

$$D_A := \partial_r \ln A, \qquad D_B := \partial_r \ln B. \tag{7.3}$$

Notice again that we use logarithmic derivatives for the lapse and the spatial metric, but only an ordinary derivative for the shift. For the extrinsic curvature, we will use the mixed components

$$K_A := K^r_r, \qquad K_B := K^\theta_\theta = K^\phi_\phi. \tag{7.4}$$

Following [31], we will change our main evolution variables and make use of the ''antitrace'' of the metric spatial derivatives $D = D_A - 2D_B$, and the trace of the extrinsic curvature $K = K_A + 2K_B$, instead of D_A and K_A.

For the regularization of the evolution equations at the origin we will follow the procedure described in [31], which requires the introduction of an auxiliary variable

$$\lambda = (1 - A/B)/r. \tag{7.5}$$

Local flatness guarantees that λ is regular and of order r near the origin. By taking $\{\alpha, A, B, d_\sigma, K, K_B\}$ as even functions at $r = 0$, and $\{\sigma, D_\alpha, D, D_B, \lambda\}$ as odd, one obtains regular evolution equations at $r = 0$.

In terms of the variables introduced above, the Hamiltonian and momentum constraints become (in vacuum)

$$0 = C_h = -\partial_r D_B + \frac{D_B}{2}\left(D + \frac{D_B}{2}\right) + A K_B(2K - 3K_B) + \frac{1}{r}(D - D_B - \lambda), \tag{7.6}$$

$$0 = C_m = -\partial_r K_B + (K - 3K_B)\left[\frac{D_B}{2} + \frac{1}{r}\right]. \tag{7.7}$$

Notice that the Hamiltonian constraint is regular, while the momentum constraint still has the term $(K - 3K_B)/r \equiv (K_A - K_B)/r$ which has to be handled with care numerically. This is not a problem as the momentum constraint does not feed back into the ADM evolution equations. On the other hand, when one adds multiples of the momentum constraint to the evolution equations in order to obtain strongly hyperbolic reformulations (as in the following

section), the regularization procedure requires some of the dynamical variables to be redefined by adding to them a term proportional to λ (see [31] for details). This redefinition, however, does not affect the characteristic structure of the system. Because of this, in the following analysis we will simply ignore this issue.

For the evolution of the lapse we will again take the Bona-Masso slicing condition, which in spherical symmetry takes the form

$$\partial_t \alpha = \alpha^2(\sigma D_\alpha - fK). \tag{7.8}$$

For the shift we will use the generalized harmonic shift condition in the form (4.4). In this case one finds

$$\gamma^{mn(3)}\Gamma^r_{mn} = \frac{D}{2A} - \frac{2}{rA}, \tag{7.9}$$

$$\gamma^{mn(3)}\Gamma^r_{mn}|_{\rm flat} = -\frac{2}{rB}. \tag{7.10}$$

Notice that in the first of these expressions we have used the Christoffel symbols for the full spatial metric $dl^2 = Adr^2 + Br^2 d\Omega^2$, while in the second we used those of the flat metric $dl^2 = dr^2 + r^2 d\Omega^2$. However, as is clear from (4.4), in both cases we have to contract indices using the full inverse metric which explains why there is a factor B in the denominator of the second expression. Using these expressions we then find

$$\Delta^r = \frac{D}{2A} - \frac{2\lambda}{A}, \tag{7.11}$$

with λ defined in (7.5) above. Our final shift condition is then regular at the origin and has the form

$$\partial_t \sigma = \alpha\left[\sigma d_\sigma - \frac{D_\alpha}{A} + h\left(\frac{D}{2A} + \sigma K - \frac{2\lambda}{A}\right)\right]. \tag{7.12}$$

It is important to mention that if we had used the original condition (3.7) instead of (4.4), we would have found that the shift evolution equation was singular. Moreover, one also finds that taking σ^θ and σ^ϕ equal to zero is consistent when using (4.4) in the sense that their respective evolution equations guarantee that they remain zero, which would not have been the case with (3.7).

Going back to the metric components A and B, we find for their evolution equations

$$\partial_t A = 2\alpha A\left[\sigma\left(D_\alpha + \frac{D}{2} + D_B\right) + d_\sigma - K + 2K_B\right], \tag{7.13}$$

$$\partial_t B = 2\alpha B\left[\sigma\left(\frac{D_B}{2} + \frac{1}{r}\right) - K_B\right]. \tag{7.14}$$

The evolution equations for D_α, d_σ, D, and D_B again follow trivially from the above equations. Finally, the ADM evolution equations for the extrinsic curvature components turn out to be

$$\partial_t K = \frac{\alpha}{A}\left\{-\partial_r D_\alpha - 2\partial_r D_B + \sigma A \partial_r K + D_\alpha\left(\frac{D}{2} - D_\alpha\right) + D_B\left(D + \frac{D_B}{2}\right) + AK^2 - \frac{2}{r}(D_\alpha - D + D_B + \lambda)\right\}, \tag{7.15}$$

$$\partial_t K_B = \frac{\alpha}{A}\left\{-\frac{\partial_r D_B}{2} + \sigma A \partial_r K_B - \frac{D_\alpha D_B}{2} + \frac{D D_B}{4} + AKK_B - \frac{1}{r}\left(D_\alpha - \frac{D}{2} + D_B + \lambda\right)\right\}. \tag{7.16}$$

Notice that these are directly the standard ADM evolution equations written in terms of $\{K, K_B\}$, with no multiples of the constraints added to them. In the next section we will consider how such adjustments affect the hyperbolicity of the full system.

B. Adjustments and hyperbolicity

In order to analyze the characteristic structure of the full system of evolution equations including the gauge conditions, we start by defining

$$u := (\alpha, \sigma, A, B, \lambda), \tag{7.17}$$

$$v := (D_\alpha, d_\sigma, D, D_B, K, K_B). \tag{7.18}$$

The system of equations can then be written in the form (5.1) and (5.2). It turns out that by doing this, one finds that the ADM evolution system introduced above is not strongly hyperbolic when $f = 1$ and/or $h = 1$. This is undesirable, as these cases correspond precisely to purely harmonic coordinates.

Following [26], in order to obtain strongly hyperbolic systems we will consider adjustments to the evolution equations of the extrinsic curvature components K and K_B of the form

$$\partial_t v_i + \sum_{j=1}^{m} A_{ij}\partial_r v_j + h_i \frac{\alpha}{A} C_h = q_i. \tag{7.19}$$

Note that we are considering only very restricted adjustments here. In particular, we do not modify the evolution equations for the D's and for d_σ. As explained in Ref. [26], this is important for the blowup analysis in the next section, as otherwise the constraints that link the D's to derivatives of the u's will fail to hold and the analysis breaks down[1]. Furthermore, for simplicity we will not consider adjustments that use the momentum constraint.

For the coefficients h_K and h_{K_B} we make the following ansatz

[1]It is in fact possible to lift this restriction, but the analysis would become more involved. Since we are mostly interested in studying the effects of the generalized harmonic shift condition here we prefer not to complicate the analysis any further.

$$h_K = -2 + b(\alpha, \sigma, A, B), \tag{7.20}$$

$$h_{K_B} = [c(\alpha, \sigma, A, B) - 1]/2. \tag{7.21}$$

With these adjustments we find that the characteristic matrix for our system of evolution equations becomes

$$\mathbf{A} = \alpha \begin{pmatrix} -\sigma & 0 & 0 & 0 & f & 0 \\ 1/A & -\sigma & -h/2A & 0 & -h\sigma & 0 \\ -2\sigma & -2 & -\sigma & 0 & 2 & -8 \\ 0 & 0 & 0 & -\sigma & 0 & 2 \\ 1/A & 0 & 0 & b/A & -\sigma & 0 \\ 0 & 0 & 0 & c/2A & 0 & -\sigma \end{pmatrix}. \tag{7.22}$$

One may now readily verify that this matrix has the following eigenvalues

$$\lambda^f_\pm = \alpha(\pm\sqrt{f/A} - \sigma), \tag{7.23}$$

$$\lambda^h_\pm = \alpha(\pm\sqrt{h/A} - \sigma), \tag{7.24}$$

$$\lambda^c_\pm = \alpha(\pm\sqrt{c/A} - \sigma). \tag{7.25}$$

The system is therefore hyperbolic for $\{f, h, c\} > 0$. Furthermore, there exists a complete set of eigenvectors as long as $c \neq f$ and $c \neq h$, so the system is strongly hyperbolic except in those two cases. The eigenfields turn out to be

$$w^f_\pm = (c - f)D_\alpha - bfD_B \pm \sqrt{fA}[(c - f)K - 2bK_B], \tag{7.26}$$

$$\begin{aligned} w^h_\pm = (c - h)\Big\{&A^{1/2}[d_\sigma - (1 \pm \sigma\sqrt{hA})K] \mp \sqrt{h}\frac{D}{2}\Big\} \\ &\pm \sqrt{h}[b(1 \pm \sigma\sqrt{hA}) - 2c]D_B \\ &+ 2\sqrt{A}[b(1 \pm \sigma\sqrt{hA}) - 2h]K_B, \end{aligned} \tag{7.27}$$

$$w^c_\pm = \sqrt{c}D_B \pm 2\sqrt{A}K_B. \tag{7.28}$$

It is clear from these expressions that when $c = f$ the first and third pairs of eigenfields become proportional to each other and are hence no longer independent, while for $c = h$ it is the second and third pairs that become proportional.

C. Gauge and constraint shocks

As we did for the 1 + 1 dimensional system, we will now study the possible formation of blowups for the evolution equations in spherical symmetry. In order to apply the source criteria for avoiding blowups we need to calculate the quadratic source terms in the evolution equations for the eigenfields. We first look for gauge shocks, for which we concentrate on the gauge eigenfields $w^f_\pm$ and $w^h_\pm$. For the quadratic source terms we find

$$c^{fff}_{\pm\pm\pm} \propto \frac{1}{(c - f)}\left(1 - f - \frac{\alpha f'}{2}\right), \tag{7.29}$$

$$c^{hhh}_{\pm\pm\pm} \propto \frac{1}{(c - h)}\frac{\partial h}{\partial \sigma}. \tag{7.30}$$

Demanding now that these terms vanish we obtain precisely the same conditions on f and h as in the 1+1 dimensional case. So again $f = 1 + \text{const.}/\alpha^2$ and $h = h(\alpha)$ are shock avoiding solutions. Furthermore, if one chooses $f = h = 1 + \text{const.}/\alpha^2$, mixed terms of the form $w^f_\pm w^h_\pm$ do not appear in the evolution equations of the gauge eigenfields $w^f_\pm$ and $w^h_\pm$, so this is a preferred choice.

In contrast to the 1 + 1 dimensional case, now also blowups associated with the constraint eigenpair $w^c_\pm$ can arise. The quadratic coefficient in this case takes the form

$$c^{ccc}_{\pm\pm\pm} \propto (1 - 4b + 3c), \tag{7.31}$$

and by asking for this coefficient to vanish we find

$$b = (1 + 3c)/4. \tag{7.32}$$

From (7.20) and (7.21) we then infer that h_K and h_{K_B} are related by

$$h_K = -1 + \frac{3h_{K_B}}{2}, \qquad h_{K_B} > -\frac{1}{2}, \tag{7.33}$$

which is the precisely the same constraint shock avoiding half line in the $\{h_K, h_{K_B}\}$ parameter space that was found in Ref. [26].

D. Numerical examples

We will now test the effects of the generalized harmonic shift in spherical symmetry by performing a series of numerical simulations. As in the 1 + 1 dimensional case, we will concentrate on two aspects, namely, the effect of the shift condition on the evolution of the metric, and the possible formation of blowups. Furthermore, in order to decouple geometric effects associated with the center of symmetry, we will consider two distinct regimes, one far from the origin and one close to it.

1. Pulses far from the origin

We will first consider simulations that are far from the origin, using initial data that is similar to the one used in Sec. VI C. We start with the Minkowski spacetime, but use a nontrivial initial slice with a profile $t_M = p(r_M)$. The initial metric and extrinsic curvature then become

$$A(t = 0) = 1 - p'^2, \tag{7.34}$$

$$B(t = 0) = 1, \tag{7.35}$$

$$K(t=0) = -\frac{1}{\sqrt{A}}\left(\frac{p''}{A} + \frac{2p'}{r}\right), \tag{7.36}$$

$$K_B(t=0) = -\frac{p'}{r\sqrt{A}}. \tag{7.37}$$

The profile function $p(r)$ is again chosen to be a Gaussian,

$$p(r) = \kappa \exp\left[-\left(\frac{r-r_c}{s}\right)^2\right], \tag{7.38}$$

using for its amplitude and width the values $\kappa = \pm 5$ and $s = 10$. The center of the Gaussian is taken at $r_c = 250$, such that for evolution times of $t \sim 100$ the perturbation will remain away from the origin.

We have performed runs with the code described in [31], which uses a method of lines with fourth order Runge-Kutta integration in time, and standard second order centered differences in space. We used 5 000 grid points and a grid spacing of $\Delta r = 0.1$ (which places the outer boundary at 500) together with a time step of $\Delta t = \Delta r/4$.

In a preparatory experiment, we studied which evolution systems perform best for our optimal gauge choice $f = h = 1$. The upper panel of Fig. 7 (which should be compared with Fig. 7 of [26]) shows the rms of the Hamiltonian constraint at time $t = 100$, as a function of the adjustment parameters h_K and h_{K_B}. We can see that the line (7.33) obtained by the source criteria is numerically preferred, although there does seem to be a discrepancy for large values of h_{K_B} for which the numerical results suggest a somewhat steeper line. This discrepancy is due to the effect of $1/r$ terms which are not taken into account by the source criteria and can be eliminated by removing these terms by hand. It is also important to point out that, in contrast to Ref. [26], the initial data used here satisfies the constraints and all subsequent constraint violations are caused by truncation error.

In order to determine which points on this line perform best, i.e. to fix the eigenspeeds $\lambda^c_\pm$ of the constraint mode, we tested different (constant) values of c. From the lower panel of Fig. 7 (to be compared with Fig. 5 of [26]) we find that values $c \sim 1/4$ and $c \gg 1$ are preferred. This observation can be readily understood by the fact that the system is not strongly hyperbolic for $c = 0$ and $c = 1$, and by the fact that for $c \sim 1$ we expect contributions from mixed source terms, since then $w^f_\pm$, $w^h_\pm$, and $w^c_\pm$ propagate with similar or even identical eigenspeeds.

For our main experiment regarding gauge effects, we concentrated on evolution systems which belong to the shock avoiding family $h_K = -1 + 3h_{K_B}/2$, where for c we considered three different values: $c = \{1/4, 1, 4\}$. As long as the pulses remain far from the origin, we have found that the evolutions behave in a very similar way to those of the 1 + 1 dimensional case described in Sec. VI C. We summarize these results in Fig. 8, showing for these three choices of c the rms of the Hamiltonian constraint at

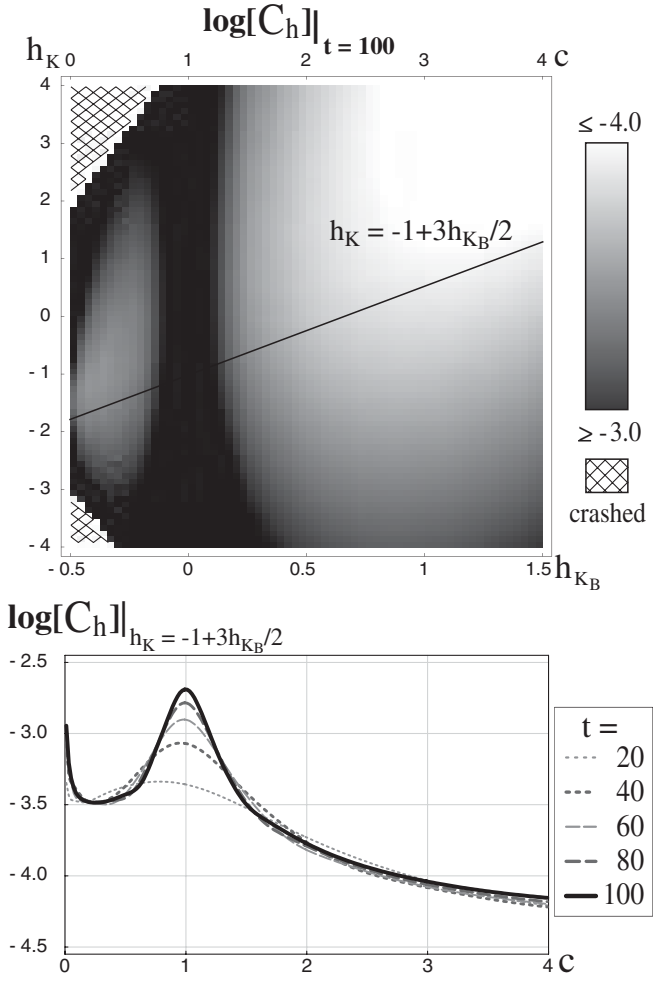

FIG. 7. Top: Contour plot of the rms of the Hamiltonian constraint at time $t = 100$ as a function of the adjustment parameters h_K and h_{K_B}. The parameter line suggested by the source criteria, $h_K = -1 + 3h_{K_B}/2$ with $h_{K_B} > -1/2$, is shown as a solid line. Bottom: For reasons described in the text, along this line $c \sim 1/4$ and $c \gg 1$ are preferred values for c, the latter determining the eigenspeeds $\lambda^c_\pm$ of the constraint modes.

time $t = 100$ as a function of f and h. These graphs are very similar to Fig. 6 and show that $f = 1$ together with $h = 1$ or $h \gg 1$, and $f = h$ are again preferred parameter choices, indicating that the same mechanisms as in the 1 + 1 dimensional case are at work. One should observe the different scales when comparing the three plots corresponding to different values of c, which indicate that by far the lowest constraint violations are found when the constraint eigenspeed is different from the gauge eigenspeeds. Notice also in the middle plot corresponding to $c = 1$ that the region around $f = h = 1$ is in fact dark. This can be explained by the fact that for $f = h = c = 1$ the evolution system is not strongly hyperbolic.

When the pulses come close to the origin, however, additional effects arise due to $1/r$ terms. In the next section we will consider this situation.

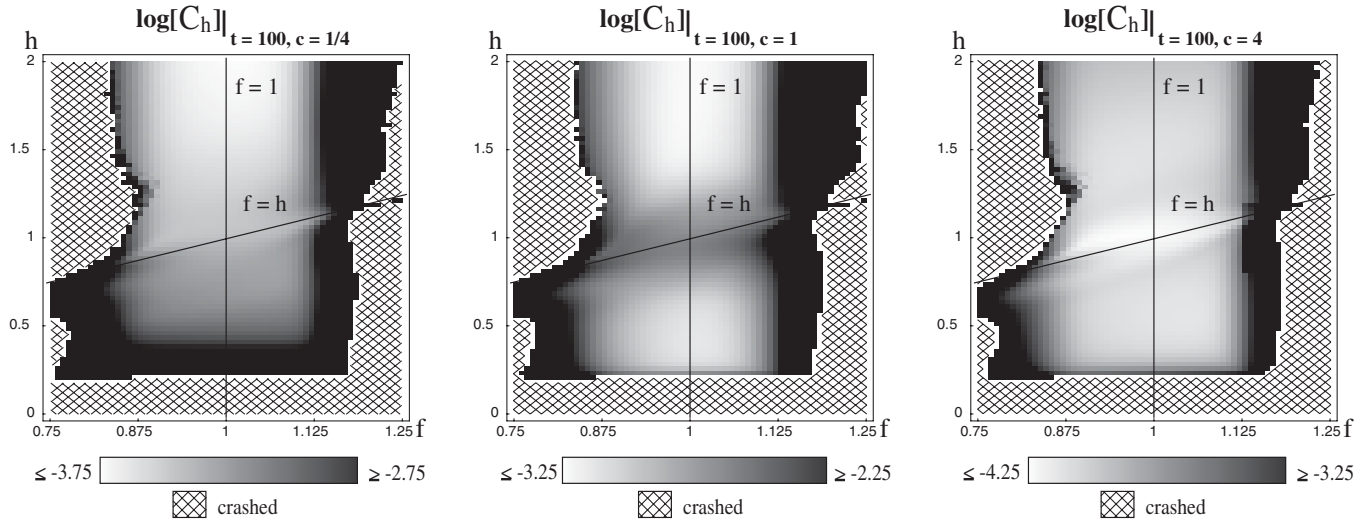

FIG. 8. Contour plot of the rms of the Hamiltonian constraint at time $t = 100$ for $c = \{1/4, 1, 4\}$. As in the $1 + 1$ dimensional case, $f = 1$ together with $h = 1$ or $h \gg 1$, and $f = h$ are preferred parameter choices. Furthermore, by far the lowest constraint violations are found when the constraint eigenspeed is different from the gauge eigenspeeds, i.e. for $c \neq 1$.

2. Pulses close to the origin

In order to see directly the effect of the generalized harmonic shift condition on the evolution of the geometric variables, we will consider again a series of simulations of Minkowski spacetime, but this time close to the origin $r = 0$. The initial data for these runs will be simpler than the one used in the previous section: We start with a flat Minkowski slice with $A = B = 1$ and $K_A = K_B = 0$, and take a nontrivial initial lapse of the form

$$\alpha = 1 + \kappa r^2 (e^{-(r-r_c)^2/s^2} + e^{-(r+r_c)^2/s^2}), \qquad (7.39)$$

with $\kappa = 10^{-5}$, $r_c = 10$, and $s = 1$ (the reason for the two Gaussians is to make sure the initial lapse is an even function of r). All simulations shown here use 4 000 grid points, with a grid spacing of $\Delta r = 0.01$ (which places the outer boundary at $r = 40$), together with a time step of $\Delta r/4$. In the plots, the initial data is shown as a dashed line and the final values at $t = 20$ as a solid line. Intermediate values are plotted every $\Delta t = 2$ in light gray.

As reference, we first show in Fig. 9 a run for the case of harmonic slicing ($f = 1$) with no shift. In order to look at the details in a clearer way, in the figure we plot $\alpha - 1$, $A - 1$, and $B - 1$. As expected, the perturbation pulse in the lapse separates into two pulses, one moving outward and one inward. The inward moving pulse goes through the origin and starts moving out much in the way a simple scalar wave would. The pulses in the lapse are accompanied by similar pulses in the metric variables A and B. However, one can clearly see that the metric variables are not evolving toward trivial values, so in the end we are left with Minkowski slices with nontrivial spatial coordinates.

Next we consider the same situation, but now using a harmonic shift with $h = 1$. Figure 10 shows results from

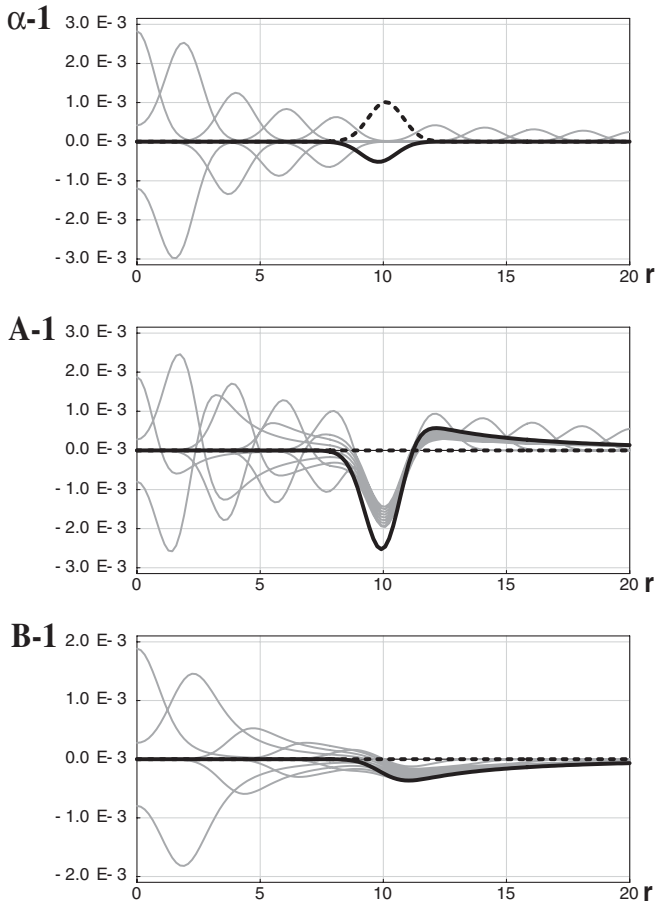

FIG. 9. Evolution of pulses close to the origin for harmonic slicing ($f = 1$) and zero shift. In order to make the details more visible, here we plot $\alpha - 1$, $A - 1$, and $B - 1$.

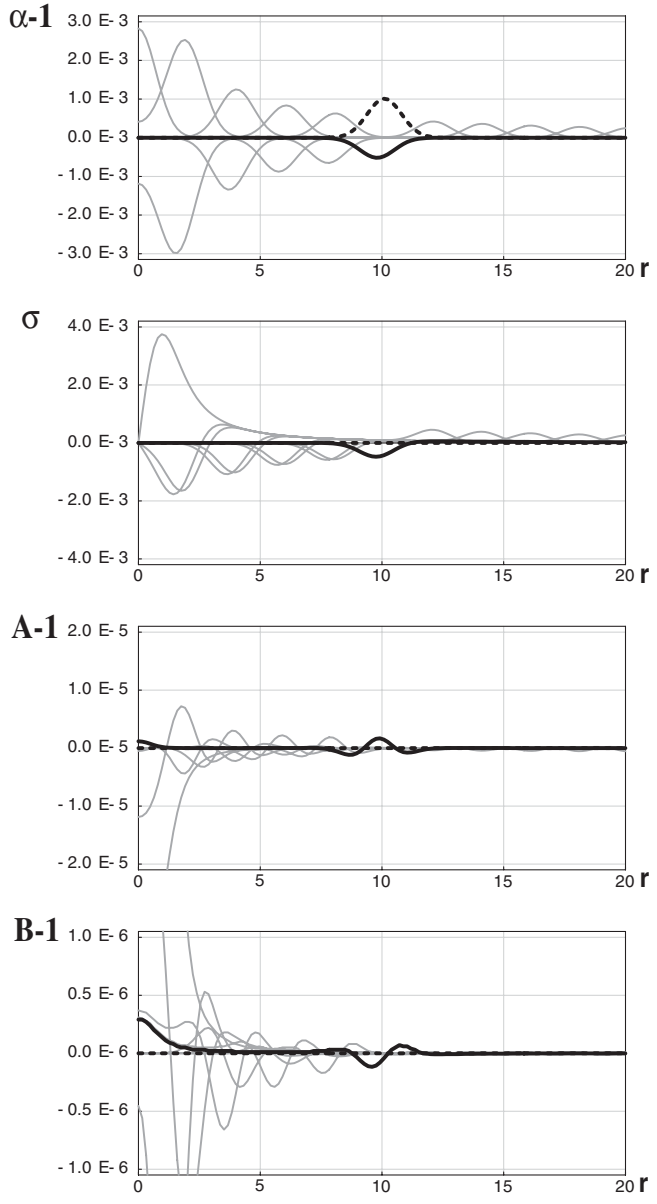

FIG. 10. As previous plot, but using the harmonic shift condition with $h = 1$.

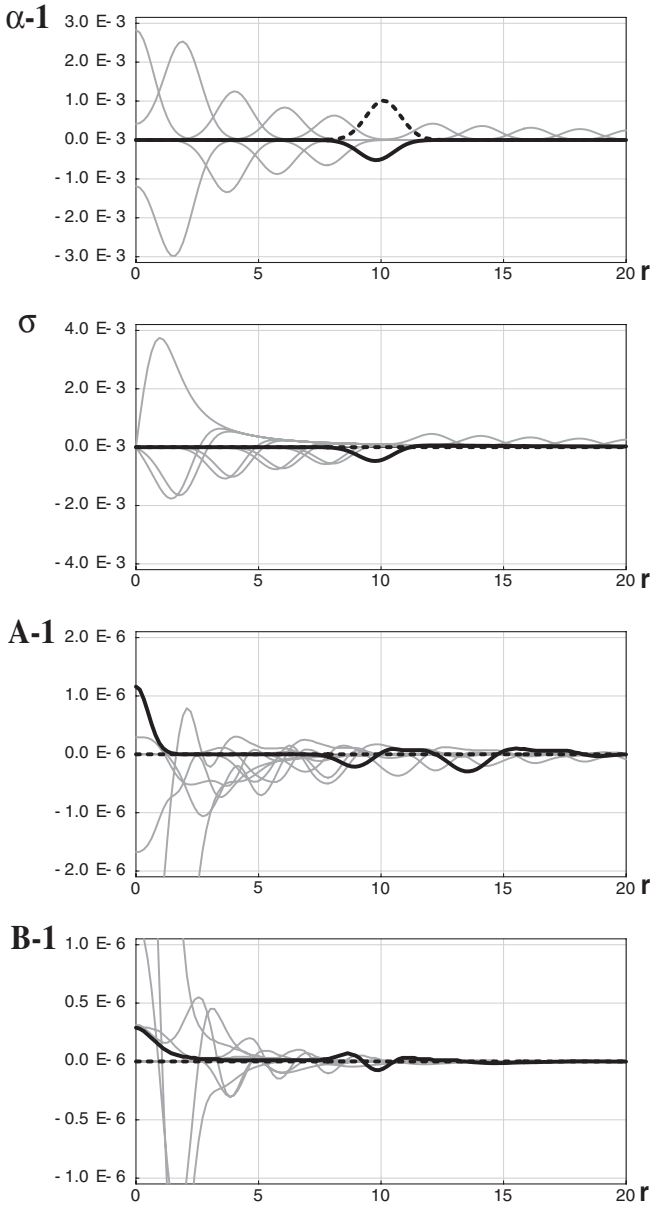

FIG. 11. Same as previous plots, but now using the generalized harmonic shift with $h = 2$. The metric coefficient A (and to a lesser extent B) shows evidence of two pulses separating and traveling at different speeds.

this run. The lapse behaves in exactly the same way as before, but now there is a nontrivial shift. The evolution of σ indicates that the shift behaves much in the same way as the lapse, with two pulses traveling in opposite directions, with the inward moving pulse going through the origin and then moving out as expected. The evolution of the metric variables A and B shows that after the ingoing pulse goes through the origin and starts moving out, the perturbations on the metric become very small. The shift then seems to be having a similar effect to the one it had in the $1 + 1$ case, making the metric components evolve toward trivial values.

Figure 11 shows a similar run, but now using $f = 1$ and $h = 2$. The whole simulation behaves much the same way as before, except for the fact that the metric coefficient A (and to a lesser extent B) now shows evidence of two pulses separating and traveling at different speeds after the rebound through the origin.

Finally, in Fig. 12 we show a simulation with $h = 1$ for a case where we have left the lapse equal to one throughout the evolution. The initial data in this case is purely Minkowski data with a shift of the form

$$\sigma = \kappa r(e^{-(r-r_c)^2/s^2} + e^{-(r+r_c)^2/s^2}), \tag{7.40}$$

with $\kappa = 10^{-3}$, $s = 1$, and $r_c = 5$. The purpose of this run is to decouple the harmonic shift condition from the slicing

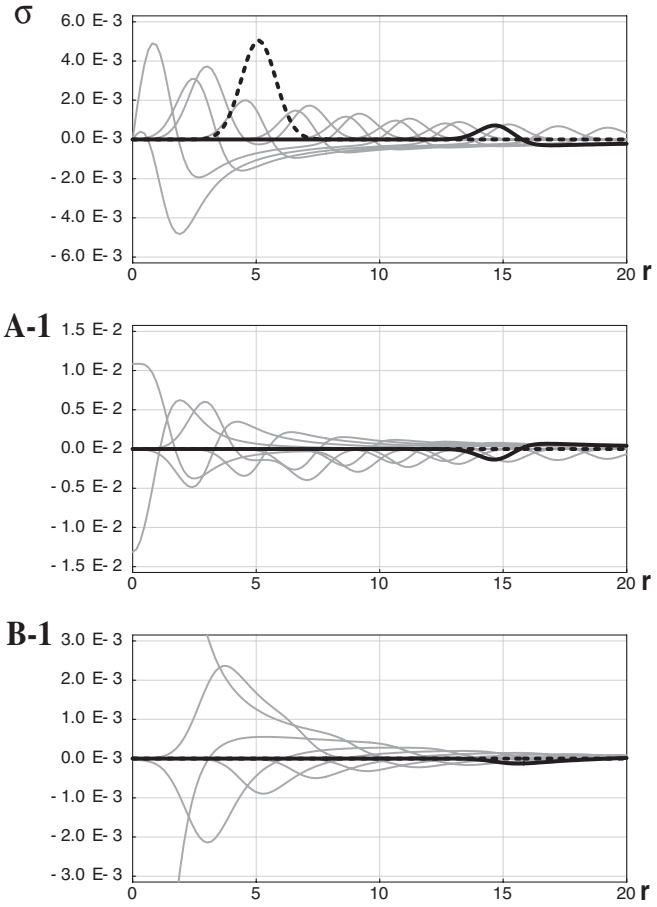

FIG. 12. Trivial Minkowski slices where the lapse remains equal to unity, together with the harmonic shift condition ($h = 1$).

condition. The figure shows clearly how, even though the initial pulse in the shift produces perturbations in the metric coefficients, these perturbations rapidly decrease in size leaving trivial values behind them.

One should mention the fact that, even though we do not show convergence plots in this section, in all cases convergence has been studied and we have found that the simulations converge at close to second order.

VIII. DISCUSSION

We have proposed a natural generalization of the condition for harmonic spatial coordinates analogous to the generalization of harmonic time slices of Bona *et al.* [19], and closely related to shift conditions recently introduced by Lindblom and Scheel [8], and by Bona and Palenzuela [22]. This coordinate condition implies an evolution equation for the shift components. We have also found that if one wants to decouple this evolution equation for the shift from the choice of slicing condition, it is important to work with a rescaled shift vector $\sigma^i = \beta^i/\alpha$.

The generalized harmonic shift condition thus obtained turns out not to be 3-covariant, which is not surprising as it involves the 3-Christoffel symbols directly. In order to be able to use this condition in arbitrary sets of curvilinear coordinates, and to be sure that we always obtain the same shift independently of the choice of spatial coordinates, we have proposed that the condition should be interpreted as always being applied to topologically Cartesian coordinates, and later rewritten in a general curvilinear coordinate system. In this way we have obtained a fully 3-covariant version of the generalized harmonic shift condition.

We have shown that the evolution equation for the shift proposed here can be seen to lead to strongly hyperbolic evolution systems both in the case of $1 + 1$ ''toy'' relativity and in the case of spherical symmetry. Though we have not done a completely general analysis here, it is to be expected that it will also lead to strongly hyperbolic systems in the 3D case. Here we have concentrated on simple one-dimensional systems in order to take the hyperbolicity analysis further and study the possible formation of blowups associated with this shift condition. We find that the coefficient h controlling the gauge speed associated with the shift can be an arbitrary function of the lapse, but must be independent of the shift itself in order to avoid blowups. In the slicing and constraint sectors we recover previous results found in [26]. An important result of this study is the fact that evolutions will be much better behaved if the gauge speeds associated with the lapse and shift are the same. This can be understood from the fact that terms in the sources that are mixed products of eigenfields associated to the lapse and shift vanish in this case. This implies that if one wants to use a shift of the generalized harmonic family, together with a lapse of the Bona-Masso type (like $1 + \log$ slicing), it is best to take $h(\alpha) = f(\alpha)$. In particular, the shock avoiding family $h = f = 1 + \text{const.}/\alpha^2$ is an optimal choice.

We have also performed a series of numerical simulations both to confirm the predictions of the blowup analysis, and to study what effect the shift has on the evolution of the geometric variables. In the 1+1 dimensional case, we find that the effect of the shift is to take the spatial metric back to a trivial value everywhere, by propagating away any nontrivial values in a wavelike fashion. In spherical symmetry the situation is considerably richer, but our main result is that when one uses the 3-covariant version of the generalized harmonic shift, then the effect of the shift is also to drive the metric coefficients to trivial values by propagating away any initial perturbations in the way one would expect for spherical waves, i.e. the perturbations become smaller as they propagate outwards. It is important to mention that, had we not used the covariant form of the shift condition and tried to apply the original noncovariant version directly to spherical coordinates, we would have found the shift condition to be singular, and worse still, to break the original spherical symmetry of the system. This shows that working with the 3-covariant version is the correct approach.

As a final comment, one should also mention the fact that the requirement of 3-covariance is not satisfied by some recently proposed shift conditions that are currently being used by large scale 3D simulations, such as the "Gamma driver" shift [4,32,33]. We are currently also studying 3-covariant versions of those conditions.

APPENDIX: GENERALIZED HARMONIC LAPSE AND SHIFT CONDITIONS

Here we will provide a general derivation of Eqs. (3.1) and (3.6) for the lapse and shift. Let us start by considering the d'Alambertian of any number a of functions $\psi^a(x^\mu)$ with their corresponding source terms

$$\Box\psi^a = S^{\psi^a}. \tag{A1}$$

Now, the d'Alambertian can be written in general as

$$\Box\psi^a = \frac{1}{\sqrt{-g}}\,\partial_\mu[\sqrt{-g}g^{\mu\nu}\partial_\nu\psi^a]. \tag{A2}$$

Using $g^{\mu\nu} = \gamma^{\mu\nu} - n^\mu n^\nu$, with $\gamma^{\mu\nu}$ the projector operator on the hypersurfaces Σ_t with normal n^μ, we find

$$\begin{aligned}\Box\psi^a = &\frac{1}{\alpha\sqrt{\gamma}}\,\partial_\mu[\alpha\sqrt{\gamma}\gamma^{\mu\nu}\partial_\nu\psi^a]\\ &- \frac{1}{\alpha\sqrt{\gamma}}\,\partial_\mu[\alpha\sqrt{\gamma}n^\mu n^\nu\partial_\nu\psi^a],\end{aligned} \tag{A3}$$

where we used the fact that $g := \det g_{\mu\nu} = -\alpha^2\gamma$ with $\gamma := \det\gamma_{ij}$ the determinant of the 3-metric on Σ_t. We then have

$$\begin{aligned}\Box\psi^a = &{}^3\Delta\psi^a + a^\mu\nabla_\mu\psi^a + Kn^\mu\nabla_\mu\psi^a\\ &- n^\mu\nabla_\mu(n^\nu\nabla_\nu\psi^a),\end{aligned} \tag{A4}$$

where ${}^3\Delta$ is the Laplacian compatible with the 3-metric γ_{ij}, $a^\mu = n^\nu\nabla_\nu n^\mu \equiv \gamma^{\mu\nu}\nabla_\nu[\ln\alpha] =: D^\mu[\ln\alpha]$ is the 4-acceleration of the normal observers, and we used $K = -\nabla_\nu n^\nu$.

In order to obtain for instance a system of first order equations one can further define

$$Q^{\mu a} := D^\mu\psi^a, \tag{A5}$$

$$\Pi^a := \mathcal{L}_{\vec{n}}\psi^a = n^\nu\nabla_\nu\psi^a, \tag{A6}$$

where $D^\mu\psi^a := \gamma^{\mu\sigma}\nabla_\sigma\psi^a$. Collecting the above results we obtain

$$\mathcal{L}_{\vec{n}}\Pi^a - a_\mu Q^{\mu a} - D_\mu Q^{\mu a} - \Pi^a K = -S^{\psi^a}. \tag{A7}$$

A simple application of the above results is the case when $\psi^a = x^a$, in which case $\Pi^a = n^a = (1, -\beta^i)/\alpha$, $Q^a_\mu = \gamma^a_\mu$, and $D_\nu Q^{\nu i} = \partial_j(\sqrt{\gamma}\gamma^{ij})/\sqrt{\gamma} \equiv -{}^{(3)}\Gamma^i$. The above equation with $S^{\psi^a} = 0$ is then called the *harmonic coordinate condition*, which provides an evolution equation for the lapse—Eq. (2.9)—and for the shift—Eq. (2.10)—when taking $x^a = (t, x^i)$ with t defining the time slicings and x^i being spatial coordinates on Σ_t.

On the other hand one can take $\Box\psi^a = S^{\psi^a}$ with a source term of the form $S^{\psi^a} = q_{\psi^a}n^\mu n^\nu\nabla_\mu\nabla_\nu\psi^a$ (no sum over index a). Now, using $n^\mu n^\nu = \gamma^{\mu\nu} - g^{\mu\nu}$, one obtains

$$n^\mu n^\nu\nabla_\mu\nabla_\nu\psi^a = \gamma^{\mu\nu}\nabla_\mu\nabla_\nu\psi^a - \Box\psi^a. \tag{A8}$$

Using the orthogonal decomposition $\nabla_\nu\psi^a = D_\nu\psi^a - n_\nu n_\sigma\nabla^\sigma\psi^a = Q^a_\nu - n_\nu\Pi^a$ we find

$$n^\mu n^\nu\nabla_\mu\nabla_\nu\psi^a = D_\nu Q^{\nu a} + \Pi^a K - \Box\psi^a, \tag{A9}$$

where we used $\gamma^{\mu\sigma}\nabla_\mu n_\sigma = \nabla_\mu n^\mu = -K$ and $\gamma^{\mu\nu}n_\nu \equiv 0$. In this way the equation $\Box\psi^a = S^{\psi^a}$ becomes

$$\Box\psi^a = \frac{q_{\psi^a}}{1 + q_{\psi^a}}(D_\nu Q^{\nu a} + \Pi^a K). \tag{A10}$$

Finally, $-\Box\psi^a$ is given by the left-hand side of Eq. (A7), from where we find

$$\begin{aligned}&\mathcal{L}_{\vec{n}}\Pi^a - a_\mu Q^{\mu a} - D_\mu Q^{\mu a} - \Pi^a K\\ &\quad = -\frac{q_{\psi^a}}{1 + q_{\psi^a}}(D_\nu Q^{\nu a} + \Pi^a K),\end{aligned} \tag{A11}$$

which simplifies to

$$\mathcal{L}_{\vec{n}}\Pi^a - a_\mu Q^{\mu a} = \frac{1}{1 + q_{\psi^a}}(D_\nu Q^{\nu a} + \Pi^a K). \tag{A.12}$$

In this way by taking $\psi^a = (t, x^i)$, $q_t = a_f = 1/f - 1$, $q_{x^i} = a_h = 1/h - 1$, together with Eqs. (A5) and (A6) (leading to $\Pi^a = n^a = (1, -\beta^i)/\alpha$ and $Q^a_\mu = \gamma^a_\mu$), one recovers the evolution Eqs. (3.1) and (3.6) for α and β^i, respectively.

ACKNOWLEDGMENTS

It is a pleasure to thank Sascha Husa for many useful discussions and comments. This work was supported in part by DGAPA-UNAM through Grants No. IN112401, No. IN122002, and No. IN119005 and by DFG Grant "SFB Transregio 7: Gravitationswellenastronomie." B. R. acknowledges financial support from the Richard-Schieber Stiftung. All runs were made at the EKBEK linux cluster in the "Laboratorio de Super-Cómputo Astrofísico (LaSumA)," CINVESTAV, built through CONACyT Grant No. 42748.

[1] L. Smarr and J. York, Phys. Rev. D **17**, 1945 (1978).
[2] L. Smarr and J. York, Phys. Rev. D **17**, 2529 (1978).
[3] O. Sarbach and M. Tiglio, Phys. Rev. D **66**, 064023 (2002).
[4] M. Alcubierre, B. Brügmann, P. Diener, M. Koppitz, D. Pollney, E. Seidel, and R. Takahashi, Phys. Rev. D **67**, 084023 (2003).
[5] M. Alcubierre, Classical Quantum Gravity **20**, 607 (2003).
[6] M. Alcubierre, A. Corichi, J. González, D. Nuñez, and M. Salgado, Classical Quantum Gravity **20**, 3951 (2003).
[7] M. Alcubierre, A. Corichi, J. González, D. Nuñez, and M. Salgado, Phys. Rev. D **67**, 104021 (2003).
[8] L. Lindblom and M. A. Scheel, Phys. Rev. D **67**, 124005 (2003).
[9] Y. Bruhat, Acta Mathematica **88**, 141 (1952).
[10] B. Szilagyi, B. Schmidt, and J. Winicour, Phys. Rev. D **65**, 064015 (2002).
[11] D. Garfinkle, Phys. Rev. D **65**, 044029 (2002).
[12] F. Pretorius, Classical Quantum Gravity **22**, 425 (2005).
[13] C. Bona and J. Massó, Phys. Rev. D **38**, 2419 (1988).
[14] C. Bona and J. Massó, Phys. Rev. D **40**, 1022 (1989).
[15] C. Bona and J. Massó, Phys. Rev. Lett. **68**, 1097 (1992).
[16] A. Abrahams, A. Anderson, Y. Choquet-Bruhat, and J. York, Phys. Rev. Lett. **75**, 3377 (1995).
[17] A. Geyer and H. Herold, Phys. Rev. D **52**, 6182 (1995).
[18] C. Bona, J. Massó, E. Seidel, and J. Stela, Phys. Rev. D **56**, 3405 (1997).
[19] C. Bona, J. Massó, E. Seidel, and J. Stela, Phys. Rev. Lett. **75**, 600 (1995).
[20] D. Bernstein, Ph.D. thesis, University of Illinois Urbana-Champaign, 1993.
[21] P. Anninos, K. Camarda, J. Massó, E. Seidel, W.-M. Suen, and J. Towns, Phys. Rev. D **52**, 2059 (1995).
[22] C. Bona and C. Palenzuela, Phys. Rev. D **69**, 104003 (2004).
[23] J. York, in *Sources of Gravitational Radiation*, edited by L. Smarr (Cambridge University Press, Cambridge, England, 1979).
[24] C. Bona and J. Massó, Int. J. Mod. Phys. C: Phys. Comput. **4**, 88 (1993).
[25] M. Alcubierre, Phys. Rev. D **55**, 5981 (1997).
[26] B. Reimann, M. Alcubierre, J. A. González, and D. Nuñez, Phys. Rev. D **71**, 064021 (2005).
[27] S. Alinhac, *Blowup for Nonlinear Hyperbolic Equations* (Birkhäuser, Boston, 1995).
[28] F. John, *Partial Differential Equations* (Springer-Verlag, New York, 1986).
[29] R. Arnowitt, S. Deser, and C. W. Misner, in *Gravitation: An Introduction to Current Research*, edited by L. Witten (John Wiley, New York, 1962), pp. 227–265.
[30] M. Alcubierre and J. Massó, Phys. Rev. D **57**, R4511 (1998).
[31] M. Alcubierre and J. González, Comput. Phys. Commun. **167**, 76 (2005).
[32] B. Brügmann, W. Tichy, and N. Jansen, Phys. Rev. Lett. **92**, 211101 (2004).
[33] M. Alcubierre *et al.*, Phys. Rev. D **72**, 044004 (2005).